JOURNAL OF THE MECHANICAL BEHAVIOR OF BIOMEDICAL MATERIALS 45 (2015) 175–182

Available online at www.sciencedirect.com

ScienceDirect

www.elsevier.com/locate/jmbbm

Research Paper

Characterization of dermal plates from armored catfish *Pterygoplichthys pardalis* reveals sandwich-like nanocomposite structure

Donna Ebenstein[a], *Carlos Calderon*[b], *Omar P. Troncoso*[b], *Fernando G. Torres*[b,*]

[a]*Biomedical Engineering Department, Bucknell University, 270 Breakiron Engineering Building, Lewisburg, PA 17837, USA*

[b]*Department of Mechanical Engineering, Pontificia Universidad Catolica del Peru, Av. Universitaria 1801, Lima 32, Peru*

ARTICLE INFO

Article history:
Received 14 October 2014
Received in revised form
31 January 2015
Accepted 1 February 2015
Available online 11 February 2015

Keywords:
Pterygoplichthys pardalis
Dermal plates
Arapaima gigas
Fish scales

ABSTRACT

Dermal plates from armored catfish are bony structures that cover their body. In this paper we characterized structural, chemical, and nanomechanical properties of the dermal plates from the Amazonian fish *Pterygoplichthys pardalis*. Analysis of the morphology of the plates using scanning electron microscopy (SEM) revealed that the dermal plates have a sandwich-like structure composed of an inner porous matrix surrounded by two external dense layers. This is different from the plywood-like laminated structure of elasmoid fish scales but similar to the structure of osteoderms found in the dermal armour of some reptiles and mammals. Chemical analysis performed using Fourier transform infrared spectroscopy (FTIR), differential scanning calorimetry (DSC) and X-ray diffraction (XRD) results revealed similarities between the composition of *P. pardalis* plates and the elasmoid fish scales of *Arapaima gigas*. Reduced moduli of *P. pardalis* plates measured using nanoindentation were also consistent with reported values for *A. gigas* scales, but further revealed that the dermal plate is an anisotropic and heterogeneous material, similar to many other fish scales and osteoderms. It is postulated that the sandwich-like structure of the dermal plates provides a lightweight and tough protective layer.

1. Introduction

Pterygoplichthys pardalis is an armoured catfish that inhabits the Amazon River. It belongs to the *Loricariidae* family, an extremely large and diverse group of American freshwater fish (Birindelli et al., 2007; Ferraris, 2007; Isbrücker, 1980; Reis et al., 2003). Fish species from the *Loricariidae* family have sucker mouths and are characterized by a depressed body covered by dermal plates. *Pterygoplichthys* are medium to moderately large fishes. Adults generally measure 30 to 55 cm (Nico et al., 2009) although their maximum size probably exceeds a total length of 70 cm (Liang et al., 2005).

Fish dermal armour appeared at the beginning of the Paleozoic era during the Ordovician period, approximately 500 million years ago (Hoedeman, 1974), and was common among these early fish (Colbert, 1955). Romer (1933) proposed

*Corresponding author.
E-mail address: fgtorres@pucp.pe (F.G. Torres).

http://dx.doi.org/10.1016/j.jmbbm.2015.02.002
1751-6161/

the hypothesis that the dermal armour served as a protection from predators. Ancient fish armour has evolved in terms of their multi-layered material structures and overall geometries (Bruet et al., 2008). Larger plates broke up into many smaller ones, the thickness of various layers decreased, and the number of layers decreased, improving the flexibility and manoeuvrability of the fish and increasing their speed (Colbert, 1955).

Most fish are covered by scales. Scales are similar to other collagen-based natural structures such as bones, teeth and mineralized tendons (Torres et al., 2008). For example, elastoid scales are plywood-like structures of closely packed collagen fibre layers reinforced with a mineral phase of calcium-deficient hydroxyapatite (Ikoma et al., 2003). By contrast, armoured catfish do not have scales but rather different types of dermal elements such as odontodes, teeth and dermal denticles, cranial dermal bones, postcranial dermal plates, or scutes (Sire and Huysseune, 2003). However, little is known about the structural, chemical and mechanical properties of individual dermal armour plates and scutes (Bruet et al., 2008).

The aim of this paper is to study the structure of *P. pardalis* plates using a materials science approach, in order to reveal the relevant structure-properties relationships that occur at the micro- and nanoscale. The properties of *P. pardalis* dermal plates have also been compared with those of *Arapaima gigas* fish scales since both are examples of collagen-hydroxyapatite nanocomposites. An improved understanding of structure-property relationships in fish dermal elements provides valuable information for the use of these systems as models for the development of bioinspired nanocomposites.

2. Experimental methods

2.1. Materials

Dermal plates (Fig. 1) from the Amazonian fish *P. pardalis* (body length 35 cm) were removed, washed and stored under standard conditions (20 °C and 80% relative humidity). Dermal plates from two specimens were used. They were around 15 mm in length and 1.5 mm in thickness. A different dermal plate was used in each individual test.

2.2. Fourier transform infrared (FTIR) spectroscopy

In preparation for FTIR analysis, the dermal plates were washed with distilled water, ground, and dried in a desiccator. Samples were prepared as KBr pellets. IR analysis was performed using a Lambda scientific FTIR-7600 (Australia) Fourier transform spectrometer. FTIR spectra were recorded at room temperature (26 °C), averaging 150 scans with a nominal resolution of 4 cm^{-1} over the frequency range of 4000 cm^{-1} to 400 cm^{-1}.

2.3. Differential scanning calorimetry (DSC)

In preparation for DSC tests, dermal plate samples were washed with distilled water, ground, and dried in a desiccator overnight. Around 10 mg of pulverized plates were loaded into sealed aluminium pans. DSC tests were performed in a Perkin-Elmer DSC 4000 (Waltham, MA) differential scanning calorimeter. Nitrogen was used as purging gas and the flow rate was controlled at 20 ml/min. For each run, samples were heated from 10 °C to 450 °C at a heating rate of 3 °C/min.

2.4. Scanning electron microscope (SEM)/energy dispersive X-ray spectroscopy (EDX)

Dermal plate samples were cleaned with ozone before placing them into the SEM. Tests were performed in a FEI-QUANTA 200 (Hillsboro, OR) SEM equipped with an energy-dispersive X-ray spectroscopy detector. Tests were carried out in low vacuum with a voltage of 30 kV and a working distance in the range of 9.9–11.2 mm.

2.5. X-ray diffraction (XRD)

X-ray diffraction analysis of all the dermal plate samples were performed in a BRUKER D8-FOCUS (Germany) diffraction system, using $K_{\alpha 1} - Cu$ ($\lambda = 1.5406$ A) radiation. Samples were analyzed over a 2θ range of 10° to 80° with a sampling interval of 0.02°. Crystallographic identification of the phases was accomplished by comparing the experimental XRD patterns to standards compiled by the Joint Committee on Powder Diffraction and Standards (JCPDS).

2.6. Nanoindentation analysis

In preparation for nanoindentation, three 3–5 mm long cross-sections from the dermal plates were cut, mounted in acrylic resin stubs, and progressively polished (using sand paper and slurries down to a 0.25 μm diamond paste) using standard polishing equipment. Nanoindentation analysis of embedded samples was performed using a Hysitron TI950 Triboindenter (Minneapolis, MN) equipped with a Berkovich tip. A minimum of 120 indents spaced by at least 15 μm were performed across the surface of each sample, targeting both matrix and filled pores. The same trapezoidal load function (load over

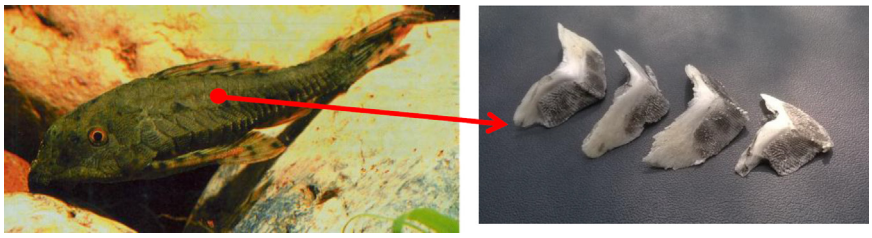

Fig. 1 – Extraction of *Pterygoplichthys pardalis* dermal plates.

10 s to a peak load of 1000 μN, hold for 30 s, and unload over 10 s) was used for all indents. Three parallel lines of indents with 15 μm spacing between lines, and spacing of 40 or 80 μm between indents within each line were also performed at several locations across each sample.

2.7. Statistical analysis

To investigate differences in mean moduli measured in each cross-section, nanoindentation results were analysed using a one-way ANOVA followed by Bonferroni post-hoc analysis at a family significance level of 0.05.

3. Results and discussion

Vertebrates present several types of external skeletal components (dermal skeleton), including osteoderms, scales, scutes, squamulae, spines and tesserae. According to Francillon-Vieillot et al. (1990) the term osteoderms refers to the mineralized plates in the dermis of amphibian, reptiles and mammals, whereas the term scale is used to describe the mineralized elements formed in the dermis. Fish scales are further classified as placoid, ganoid, cosmoid and elasmoid scales, among others (Yang et al., 2013a, 2013b). According to Sire and Huysseune (2003), the term scutes is used for the postcranial dermal plates of armoured catfish (Callichthyidae, Loricariidae, Doradidae, among others). These dermal plates are composed of osseous tissue and are similar to the osteoderms that occur in some reptiles and mammals (Francillon-Vieillot et al., 1990).

The *P. pardalis* dermal plates are different in appearance from elasmoid fish scales, which are thin flat osseous plates. Dermal plates from *P. pardalis* are not flat but have a three dimensional "V" shape. They are around 15 mm in length and 1.5 mm in thickness, having an aspect ratio (=total length/thickness) of 10 and a degree of imbrication (=exposed length/total length) of 0.50 (Fig. 2). The internal surface, which is not in contact with water, has a smooth texture. By contrast, the external surface has a rough texture due to the presence of tubercles (Song et al., 2010). A more detailed view of the periodic arrays of hemispherical tubercles can be observed in Fig. 3 (arrows). According to Sire et al. (2009), these tubercules are found on the scutes of armoured catfish (*callichthyids, loricariids* and *doradids*) and are referred to as dermal denticles, which are tooth-like elements. These characteristics are consistent with the function of the outer layer of the dermal armour, which serves as protection against predators. Song et al. (2010) reported that the presence of tubercles on the external surface has implications for both penetration resistance and hydrodynamics. The penetrating tooth of a predator would have to indent or bend the tubercles first in order to penetrate the external layer of the dermal plates, and the tubercles also modify viscous drag forces, surface shear stress and skin friction.

Fig. 2 also shows a schema of the hierarchical structure of the dermal plates of *P. pardalis*. The dermal plates present in this specimen show a sandwich-like structure, characterized

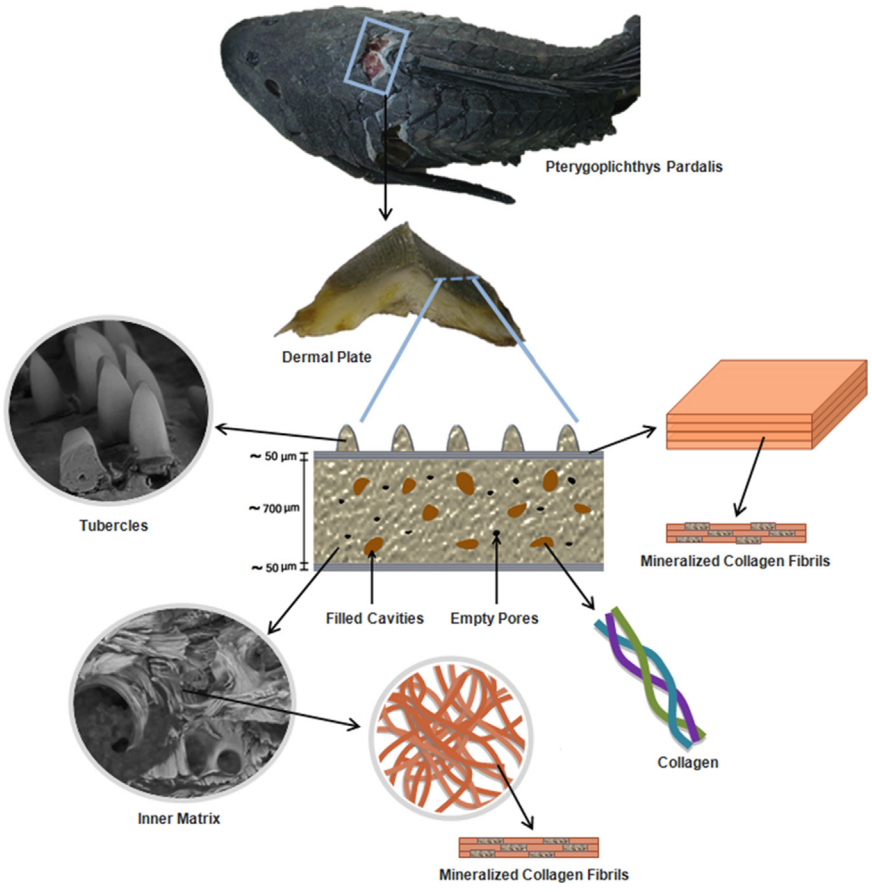

Fig. 2 – Hierarchical structure of the dermal armor of *P. pardalis*.

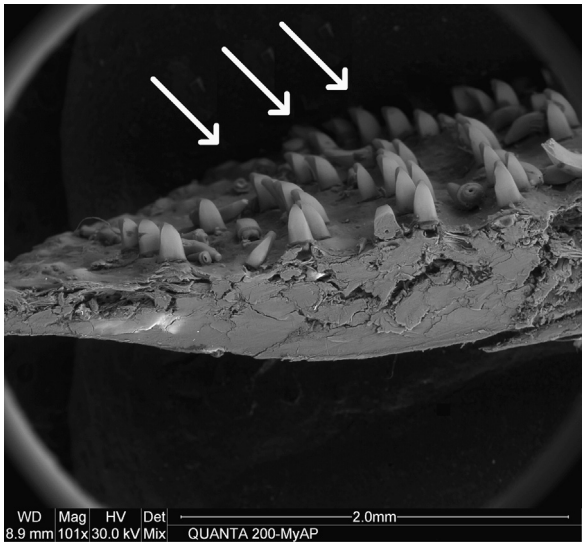

Fig. 3 – Scanning electron microscopy (SEM) image of a cross-sectional.

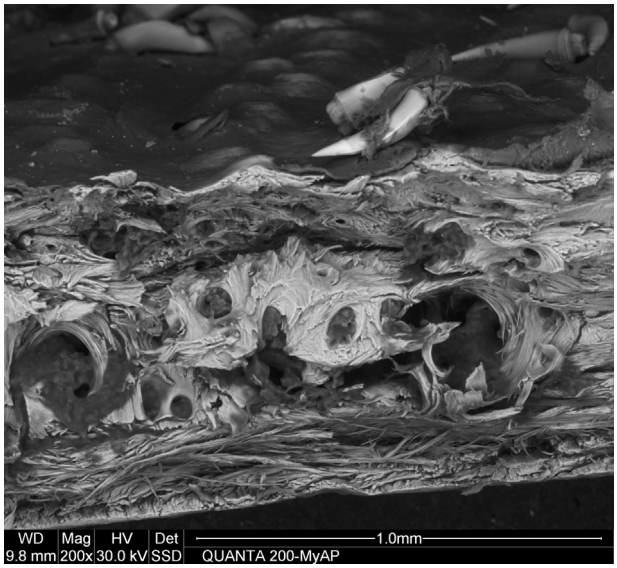

Fig. 4 – Scanning electron microscopy (SEM) image of a cross-sectional view of the internal layer of *P. pardalis* dermal plate.

by external and internal laminated layers (around 50 μm in thickness) of mineralized collagen fibrils surrounding an inner porous matrix (around 700 μm in thickness) of disorganized mineralized collagen fibrils (Fig. 4).

Two types of pores can be observed in the inner porous matrix. The smaller group of pores (~30 μm) appear to be empty while the other types of cavities (bigger pores, ~70 μm) are filled with some type of proteinaceous material, as illustrated by the EDX results in Fig. 5. The EDX results showed that the material inside the filled cavity is mainly composed of carbon (81 wt%), with a minimum percentage of calcium (3 wt%). On the other hand, the inner matrix is composed of 58 wt% of carbon, 14 wt% of oxygen, 7 wt% of phosphorus and 20 wt% of calcium (Fig. 6). This suggests that the cavities are filled with some type of protein material, because of the high presence of carbon and low presence of calcium, which is different from the highly mineralized material that forms the inner matrix itself.

The pores seem to be surrounded by concentric layers (Fig. 4) of lamellar bone. These pores are similar to the pores found in the dermal plates of alligators, which also show a porous internal structure with round pores surrounded by concentric lamellar ring layers (Chen et al., 2014). According to Yang et al. (2013a), mechanical properties of bony scales and osteoderms are dependent on the degree of porosity, with modulus and strength decreasing with increasing porosity. This will likely also apply in the case of *P. pardalis*, given that there are different kinds of pores present in the inner matrix.

A similar sandwich structure of dense outer layers surrounding a porous core are found in bony structures in many animals and locations, including turtle shell (Achrai and Wagner, 2013), armadillo osteoderms (Yang et al., 2013a), alligator osteoderms (Sun and Chen, 2013), as well as skull and rib bones (Yang et al., 2013a). This geometry is thought to provide low density combined with bending stiffness and the ability to absorb energy (Yang et al., 2013a; Sun and Chen, 2013), beneficial attributes for a light-weight catfish armor.

The sandwich nanocomposite structure of the dermal plates studied here, while similar to some osteoderms, is rather different from the structure of elasmoid fish scales which present a plywood-like laminated morphology formed by multiple collagen layers reinforced with hydroxyapatite. For instance, scales from *A. gigas* are around 1 mm in thickness and are made up of collagen layers that range from 40 to 100 μm in thickness (Torres et al., 2014).

In spite of the morphological differences, the dermal plates studied here have similarities in chemical and mechanical properties with fish scales. Both of these dermal armours combine the functions of protection, flexibility and toughness (Chen et al., 2012), which explains the similarities in characteristics. For instance, the FTIR spectra of representative *P. pardalis* dermal plates and *A. gigas* scales (depicted in Fig. 7) both show the characteristic organic absorption bands of amide I (1654 cm^{-1}), amide II (1457 cm^{-1}) and amide III (1245 cm^{-1}) (Ikoma et al., 2003; Aluigi et al., 2007; Yang et al., 2014), indicative of the presence of collagen. The inorganic content of both the *A. gigas* scale and the *P. pardalis* dermal plate are associated with the hydroxyapatite absorption bands at 559 and 1026 cm^{-1} (phosphate groups), consistent with hydroxyapatite.

The X-ray diffractograms of *P. pardalis* dermal plates and *A. gigas* scales also show striking similarities (Fig. 8). Both spectra show similar peaks at $2\theta = 25.9^{\circ}$, 32.2°, 39.4°, 47.3°, 49.3° and 53.4° corresponding to the apatite structure (Ikoma et al., 2003). These XRD results are in agreement with the previous results of tests performed on fish scales (Ikoma et al., 2003; Lin et al., 2011; Torres et al., 2008). In addition, representative thermograms of a *P. pardalis* dermal plate and a *A. gigas* scale sample (Fig. 9) reveal the same three endothermic peaks at 77 °C, 213 °C and 306 °C. The first peak is related to the collagen denaturation process, the second peak is associated with the melting and decomposition of collagen, and the third peak is related to thermal degradation of collagen (Uskokovic et al., 2003).

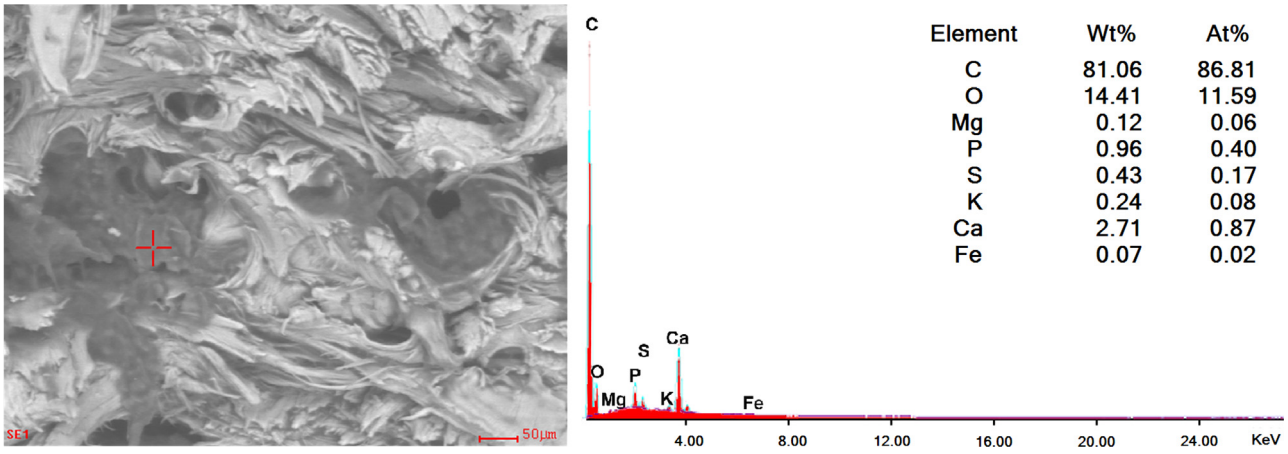

Element	Wt%	At%
C	81.06	86.81
O	14.41	11.59
Mg	0.12	0.06
P	0.96	0.40
S	0.43	0.17
K	0.24	0.08
Ca	2.71	0.87
Fe	0.07	0.02

Fig. 5 – EDX analysis of filled porous from *P. pardalis* dermal plate.

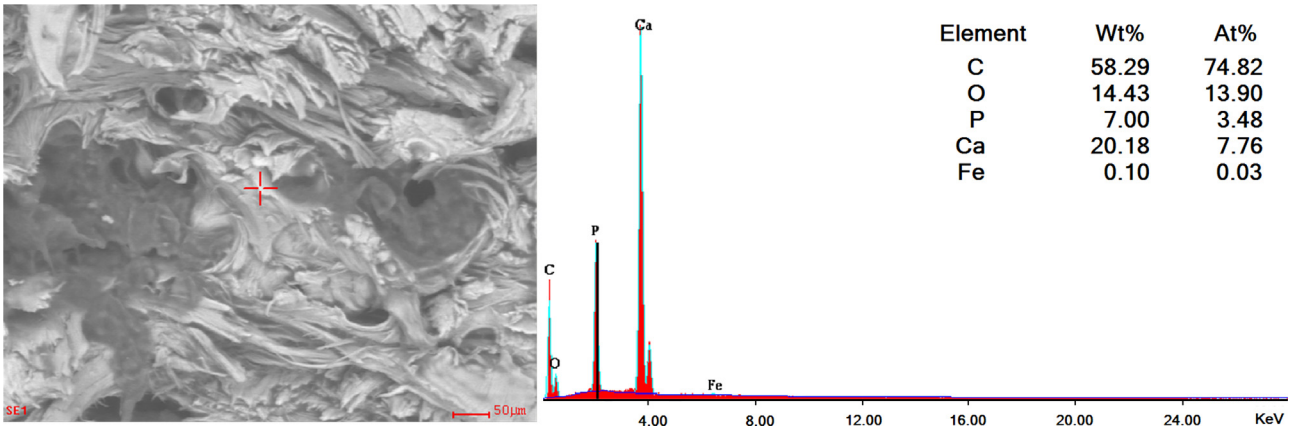

Element	Wt%	At%
C	58.29	74.82
O	14.43	13.90
P	7.00	3.48
Ca	20.18	7.76
Fe	0.10	0.03

Fig. 6 – EDX analysis of inner structure porous matrix from *P. pardalis* dermal plates.

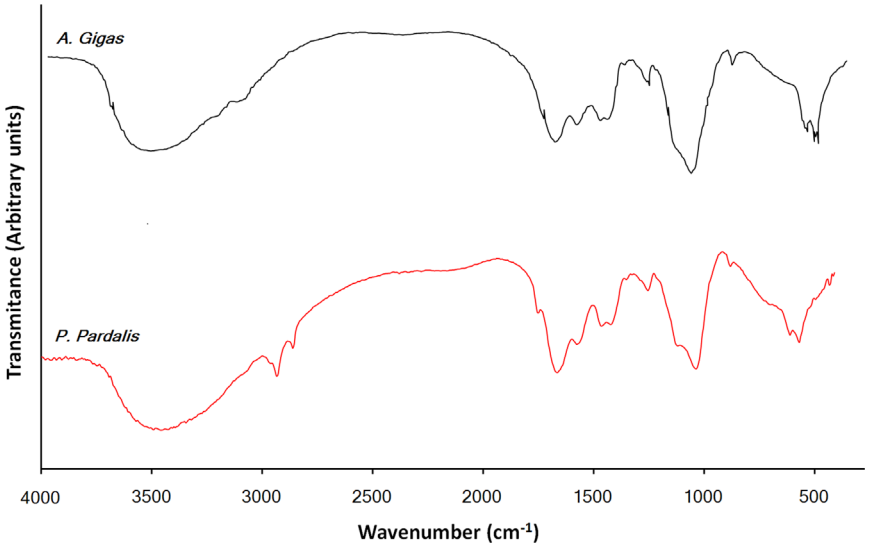

Fig. 7 – FTIR spectra of *Arapaima gigas* scales (adapted from Torres et al., 2008) and *P. pardalis* dermal plates.

Together, these analyses suggest that *P. pardalis* dermal plates have similar composition to *A. gigas* scales, being composed of mineralized collagen fibrils in a bony structure. Since most dermal armours, including fish scales and osteoderms, include a bony layer (Yang et al., 2013a), the chemical composition, being primarily collagen and hydroxyapatite, is a reasonable result. Combined with the microstructural analysis (Fig. 4), it seems likely that the outer layers are composed of lamellar (parallel-fibered) bone while the inner porous matrix is composed of a mix of porous and dense

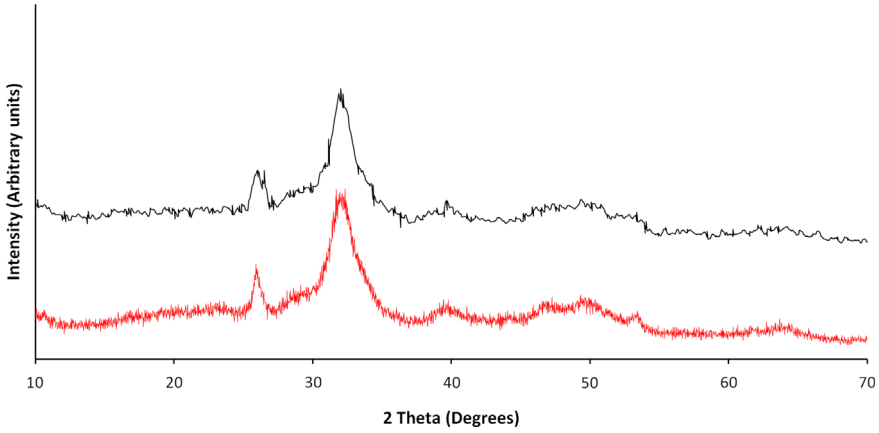

Fig. 8 – XRD diffractogram of *A. gigas* scales (adapted from Torres et al., 2008) and *P. pardalis* dermal plates.

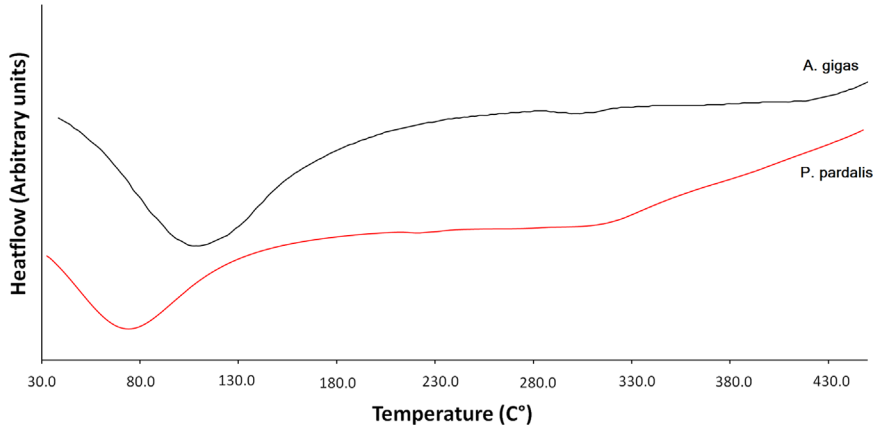

Fig. 9 – DSC thermogram of *A. gigas* scales (adapted from Torres et al., 2012) and *P. pardalis* dermal plates.

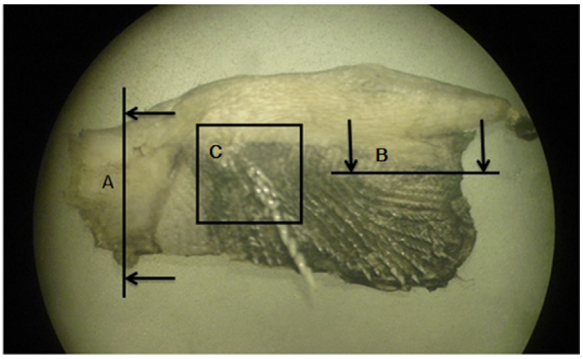

Fig. 10 – Illustration of three sections cut, embedded and polished for nanoindentation testing.

bone, with lamellar rings around the pores, and with varying degrees of mineralization.

Fig. 10 shows the three sections analysed by nanoindentation. The reduced modulus (E_r) values for the matrix, including indents from all three sections, ranged from 4.4 to 31.4 GPa, with an overall mean and standard deviation of 15.6±5.5 GPa. This result is in good agreement with nanoindentation tests carried out on fish scales. For instance, Torres et al. (2014) found E_r ranging 5–30 GPa for *A. gigas* scales, Chen et al. (2012) obtained 15.7±5.1 for the internal regions of *A. gigas* scales, and Lin et al. (2011) reported 16.7±4.0 GPa for the internal regions of *A. gigas* scales. Polishing removed more material from the filled pores than from the surrounding matrix or embedding resin, suggesting that the less mineralized material filling the pores has a lower hardness than the mineralized matrix, as expected based on the chemical analysis. However, the increased wear resulted in rough, irregular surfaces in the pores that lead to inconsistent mechanical property assessment using nanoindentation, so the modulus of the material filling the pores could not be accurately measured.

Table 1 – Matrix reduced modulus values for each section reported as mean±standard deviation. The number of indents averaged in each section is also reported (*n*).

Section	E_r (GPa)	*n*
A	21.0±4.2	108
B	16.2±3.9	67
C	11.3±2.3	150

Matrix modulus values by section (Table 1) show regional variations in modulus, with reduced moduli ranging from 11.3±2.3 to 21.0±4.2 in different sections, in fairly good agreement with nanoindentation tests carried out on osteoderms. For example, alligator osteoderms were found to have

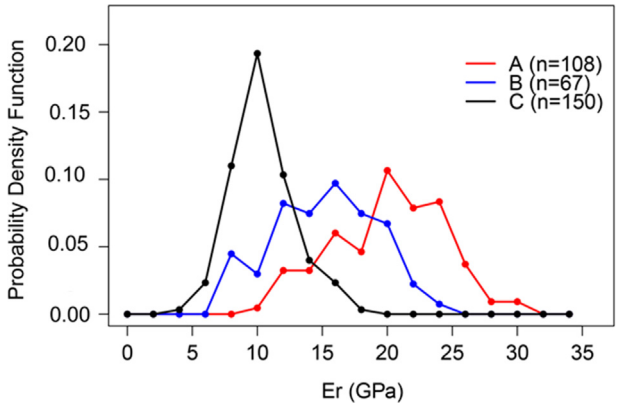

Fig. 11 – Distribution of E_r values measured in the three different cross-sections.

reduced moduli ranging from 13.9±2.1 GPa to 20.3±3.4 GPa in different regions (Sun and Chen, 2013), while a turtle shell had moduli ranging from 13.8±1.9 to 20.0±2.0, also varying with region and orientation (Achrai and Wagner, 2013).

The large standard deviation of the matrix E_r values could be due to the fact that the dermal plates do not present a homogeneous structure. The matrix modulus values by section shown in Table 1 suggest that the matrix is anisotropic, with the mean E_r perpendicular to the plate (section C), being significantly lower than the mean E_r within the plane of the plate (sections A, B) ($p<0.001$). The mean reduced moduli of different sections within the plate were also significantly different ($p<0.001$), suggesting additional orientation or location related variations in modulus. Similarly, Yang et al. (2014) reported that in-plane anisotropy exists in both the cycloid and ctenoid scales, and anisotropy in mechanical properties has been reported in alligator osteoderms (Sun and Chen, 2013) and turtle shells (Achrai and Wagner, 2013). The density functions in Fig. 11 support the conclusion of anisotropy, and further illustrate that there can also be significant variability in matrix modulus within a given cross-section. These local inhomogeneities could be due to regional differences in fiber orientation, as seen in Fig. 4, regional differences in the degree of matrix mineralization, or differences in proximity to pores beneath the surface.

In fish, dermal armour is designed to be lightweight, flexible and tough (Yang et al., 2014). In *P. pardalis*, this combination of properties comes from overlapping layers of dermal plates with a sandwich structure containing a porous inner matrix. This sandwich structure is similar to the microstructure of osteoderms found in some reptiles and mammals (Yang et al., 2013a). Hence, similar deformation mechanisms likely apply. The porous inner matrix decreases the density of the dermal plate, thereby making it more lightweight. The porous inner matrix also provides a toughening mechanism, the ability to absorb energy by deformation of the less stiff (more porous) cellular foam, thereby preventing fracture of the outer lamellar layers (Sun and Chen, 2013). Flexibility is achieved by arranging these plates in overlapping layers, a structure that is also implemented in some military armour (Yang et al., 2013a). The attachment of these individual plates by nonmineralized collagen can also help dissipate energy under low loads (Sun and Chen, 2013), further enhancing the toughness and flexibility of the armour.

4. Conclusions

P. pardalis is usually a bottom-dwelling fish, which explains its lateral and top strong dermal armour in order to protect itself from predators, such as aquatic snakes, freshwater turtles, large catfishes and other predatory fishes (Nico, 2010). The dermal plates from *P. pardalis* have been characterized using a materials science approach and compared to scales from *A. gigas*. The morphology of the dermal plates is different from the *A. gigas* fish scale morphology. While scales from *A. gigas* are laminated composites (with layers 40–100 μm in thickness), dermal plates have a sandwich-like structure with an inner porous matrix (around 700 μm in thickness) sandwiched between external and internal laminated layers (around 50 μm in thickness) more comparable to osteoderms.

However, infrared spectroscopy, X-ray spectroscopy and thermal analysis by differential scanning calorimetry revealed chemical similarities between *P. pardalis* dermal plates and scales from *A. gigas*. This can be accounted for by the fact that they are both composed primarily of collagen and hydroxyapatite in a bony structure. The nanoindentation results are also in good agreement with nanoindentation tests carried out on fish scales from *A. gigas*, exhibiting a similar range and overall average reduced modulus. Detailed analysis of the nanoindentation results further shows that the average value of the reduced modulus depends on the orientation of the surface where the modulus is measured, suggesting that the dermal plates are anisotropic, similar to many other fish scales and osteoderms.

Based on comparisons to other studied organisms, it seems likely that the *P. pardalis* dermal plates provide protection through a variety of mechanisms. The tubercles on the outer surface help prevent predator tooth penetration, while the porous inner matrix can deform to help absorb energy during an attack, increasing the toughness of the dermal plate to prevent fracture and penetration to the soft tissue.

Acknowledgements

The authors would like to thank the Peruvian Science and Technology Program (FINCyT, Peru), the TWAS (Italy) and the Vice-Rectorate for Research of the Pontificia Universidad Catolica del Peru (VRI-PUCP) for financial support. Experimental aid from Mr. D. De la Torre and Mr. P. Aquino is also acknowledged. The nanoindenter used in this study was obtained through the support of the National Science Foundation (MRI-1040319). Conclusions and recommendations expressed in this paper are those of the authors and do not necessarily reflect the views of the National Science Foundation.

REFERENCES

Achrai, B., Wagner, H.D., 2013. Micro-structure and mechanical properties of the turtle carapace as a biological composite shield. Acta Biomater. 9 (4), 5890–5902.

Aluigi, A., Zoccola, M., Vineis, C., Tonin, C., Ferrero, F., Canetti, M., 2007. Study on the structure and properties of wool keratin regenerated from formic acid. Int. J. Biol. Macromol. 41, 266–273.

Birindelli, J.L., Zanata, A.M., Lima, F.C., 2007. Hypostomus chrysostiktos, a new species of armored catfish (Siluriformes: Loricariidae) from rio Paraguaçu, Bahia State, Brazil. Neotrop. Ichthyol. 5, 271–278.

Bruet, B.J., Song, J., Boyce, M.C., Ortiz, C., 2008. Materials design principles of ancient fish armour. Nat. Mater. 7, 748–756.

Chen, P.Y., Schirer, J., Simpson, A., Nay, R., Lin, Y.S., Yang, W., Lopez, M.I., Li, J., Olevsky, E.A., Meyers, M.A., 2012. Predation versus protection: fish teeth and scales evaluated by nanoindentation. J. Mater. Res. 27, 100–112.

Chen, I.H., Yang, W., Meyers, M.A., 2014. Alligator osteoderms: mechanical behavior and hierarchical structure. Mater. Sci. Eng., C 35, 441–448.

Colbert, E.H., 1955. Evolution of the Vertebrates: A History of the Backboned Animals Through Time. Wiley, New York.

Ferraris, C.J., 2007. Checklist of catfishes, recent and fossil (Osteichthyes: Siluriformes), and catalogue of siluriform primary types. Zootaxa 1418, 1–628.

Francillon-Vieillot, H., De Buffrénil, V., Castanet, J.D., Géraudie, J., Meunier, F.J., Sire, J.Y., Zylberberg, L., De Ricqlès, A., 1990. Microstructure and mineralization of vertebrate skeletal tissues. Skeletal Biomineralization: Patterns, Processes and Evolutionary Trends, 471-530.

Hoedeman, J.J., 1974. Naturalists Guide to Fresh Water Aquarium Fish. Sterling Publishing Co., Oak Tree Press Co., New York, London, and Sydney.

Ikoma, T., Kobayashi, H., Tanaka, J., Wals, D., Mann, S., 2003. Microstructure, mechanical, and biomimetic properties of fish scales from Pagrus major. J. Struct. Biol. 142, 327–333.

Isbrücker, I.J., 1980. Classification and Catalogue of the Mailed Loricariidae (Pices, Siluriformes). Versi Techn. Gegevens, Univ. van Amsterdam 22, 1-181.

Liang, S.H., Wu, H.P., Shieh, B.S., 2005. Size structure, reproductive phenology, and sex ratio of an exotic armored catfish (*Liposarcus multiradiatus*) in the Kaoping River of Taiwan. Zool. Stud. 44, 252–259.

Lin, Y.S., Wei, C.T., Olevsky, E.A., Meyers, M.A., 2011. Mechanical properties and the laminate structure of *Arapaima gigas* scales. J. Mech. Behav. Biomed. Mater. 4, 1145–1156.

Nico, L.G., 2010. Nocturnal and diurnal activity of armored suckermouth catfish (Loricariidae: Pterygoplichthys) associated with wintering Florida manatees (Trichechus manatus latirostris). Neotrop. Ichthyol. 8 (4), 893–898.

Nico, L.G., Jelks, H.L., Tuten, T., 2009. Non-native Suckermouth armored catfishes in Florida: description of nest burrows and burrow colonies with assessment of shoreline conditions. Aquat. Nuis. Spec. Res. Prog. Bull. 09–1, 1–31.

Reis, R.R., Kullander, S.O., Ferraris, C.J., 2003. Check List of Fresh Water Fishes of South and Central America. Edipucrs, Porto Alegre, Brazil.

Romer, A.S., 1933. Eurypterid influence on vertebrate history. Science 78, 114–117.

Sire, J.Y., Huysseune, A.N., 2003. Formation of dermal skeletal and dental tissues in fish: a comparative and evolutionary approach. Biol. Rev. 78, 219–249.

Sire, J.Y., Donoghue, P.C., Vickaryous, M.K., 2009. Origin and evolution of the integumentary skeleton in non-tetrapod vertebrates. J. Anat. 214 (4), 409–440.

Song, J., Reichert, S., Kallai, I., Gazit, D., Wund, M., Boyce, M.C., Ortiz, C., 2010. Quantitative microstructural studies of the armor of the marine threespine stickleback (*Gasterosteus aculeatus*). J. Struct. Biol. 171, 318–331.

Sun, C.-Y., Chen, P.-Y., 2013. Structural design and mechanical behaviour of alligator (Alligator mississippiensis) osteoderms. Acta Biomater. 9, 9049–9064.

Torres, F.G., Le Bourhis, E., Troncoso, O.P., Llamoza, J., 2014. Structure-property relationships in *Arapaima Gigas* scales revealed by nanoindentation tests. Polym. Polym. Compos. 22, 369–373.

Torres, F.G., Troncoso, O.P., Amaya, E., 2012. The effect of water on the thermal transitions of fish scales from *Arapaima Gigas*. Mater. Sci. Eng., C 32, 2212–2214.

Torres, F.G., Troncoso, O.P., Nakamatsu, J., Grande, C.J., Gomez, C.M., 2008. Characterization of the nanocomposite laminate structure occurring in fish scales from *Arapaima Gigas*. Mater. Sci. Eng., C 28, 1276–1283.

Uskokovic, V., Ignjatovic, N., Petranovic, N., 2003. Synthesis and characterization of hydroxyapatite-collagen biocomposite materials. Mater. Sci. Forum 413, 269–274.

Yang, W., Chen, I.H., Gludovatz, B., Zimmermann, E.A., Ritchie, R.O., Meyers, M.A., 2013a. Natural flexible dermal armor. Adv. Mater. 25 (1), 31–48.

Yang, W., Gludovatz, B., Zimmermann, E.A., Bale, H.A., Ritchie, R.O., Meyers, M.A., 2013b. Structure and fracture resistance of alligator gar (*Atractosteus spatula*) armored fish scales. Acta Biomater. 9 (4), 5876–5889.

Yang, W., Sherman, V., Gludovatz, B., Mackey, M., Zimmermann, E.A., Chang, E.H., Schaible, E., Qin, Z., Buehler, M., Ritchie, R., Meyers, M.A., 2014. Protective role of *Arapaima gigas* fish scales: structure and mechanical behavior. Acta Biomater. 10 (8), 3599–3614.